ACS–Based Dynamic Optimization for Curing of Polymeric Coating

Jie Xiao, Jia Li, Qiang Xu, and Yinlun Huang
Dept. of Chemical Engineering and Materials Science, Wayne State University, Detroit, MI 48202

Helen H. Lou
Dept. of Chemical Engineering, Lamar University, Beaumont, TX 77710

DOI 10.1002/aic.10750
Published online December 15, 2005 in Wiley InterScience (www.interscience.wiley.com).

Clearcoat filmbuild is a main concern for coating quality in automotive paint shops. In operation, a thin layer of clearcoat is sprayed on the top of other thin films on the vehicle surface and then baked in an oven for solvent removal, film topology finalization, and crosslinking reactions completion. Because of the complexity of physical and chemical phenomena occurring in operation and the lack of on-line measurement of key process and product parameters, ovens are always operated considerably less than optimally in terms of coating quality and energy consumption. In this report, a dynamic model-embedded ant colony system–based optimization methodology is introduced to tackle this sophisticated industrial problem. It is shown that, by comparing with a traditional Genetic Algorithm, the proposed methodology can provide better solution with reasonable computational effort. A major contribution of this work is that—probably for the first time—the oven energy minimization (process performance) can be achieved based on rigorous coating quality (product performance) constraints in a dynamic domain. This work advances coating quality control from traditional postprocess inspection-based practice (a reactive approach) to in-process on-line defect prevention–focused strategy (a proactive approach). It also provides a scientific basis for redesigning quality-guaranteed energy-efficient ovens. The methodology is, in general, applicable to a variety of industrial dynamic optimization problems, where product and process performance should be simultaneously considered. © 2005 American Institute of Chemical Engineers *AIChE J,* 52: 1410–1422, 2006

Keywords: clearcoat, curing, ant colony system, dynamic optimization, energy reduction, quality control

Introduction

Automotive coating operations involve the development of several thin layers of polymeric coatings, such as phosphate, electrocoat, powder, basecoat, and clearcoat on vehicle surface. The filmbuild of basecoat and clearcoat, usually known as topcoat, is of utmost importance to the appearance and durability of the vehicle coatings.[1] Topcoat baking, after paint spray, is critical to coating surface topology, defect prevention, and crosslinking completeness. It is recognized that oven baking is one of the most difficult operations because most of the process and product parameters are either not measurable or measured only scarcely and, more seriously, the dynamic changes of the chemical and physical properties of the topcoat are basically unknown in operation. To date, oven operational settings and their adjustment have been almost all experience based.[2]

Q. Xu is currently with the Dept. of Chemical Engineering, Lamar University, Beaumont, TX 77710.
Correspondence concerning this article should be addressed to Y. Huang at yhuang@wayne.edu.

Topcoat baking is a reactive drying operation. In an oven, radiation and convection provide heat to the thin film, which is wet initially. The solvent contained in the film is then removed by heat; consequently, the film thickness is reduced and film topology is finalized. Meanwhile, crosslinking reactions take place and finally the dry film with desired properties is developed. The ovens are the most energy-intensive units in paint shops. Today's oven design and operation technologies have already given rise to much lower energy cost than ever. It is widely recognized, however, that oven energy consumption is still much higher than it should be. A major concern for energy reduction is the assurance of coating quality. Industrial practice has shown that coating quality control (QC) has been reactive in nature, given that it relies mainly on postprocess inspection. The identified quality problems are analyzed and then, hopefully, correlated to design and/or operation parameters based on experience. Conceivably, this type of QC is ineffective. The most desirable approach for QC should be defect prevention oriented.[3] This requires the translation of quality criteria into design- and operation-related constraints. This proactive QC principle will allow simultaneous achievement of optimal process performance and product performance.

A typical reactive drying process/product optimization problem can be stated as follows: given a specific multistage oven, a desired production rate, and initial and final coating specifications, determine optimal operation parameters so that energy consumption can be minimized, all the while ensuring the coating quality. Understandably, this dynamic optimization is very complicated. This is also a generic problem that needs to be solved in three successive steps: process and product characterization, optimization formulation, and solution derivation.

The dynamic aspects of the reactive drying process and the properties of the coating product are the key concerns in quality control and process improvement. If the dynamic correlation between the process and the product is fully and precisely established, then the opportunities for energy reduction and quality assurance can be readily identified. Over the past years, vigorous attempts have been made to model the oven-baking process.[4-8] Nevertheless, most efforts were at the laboratory level, by the study of curing small sample pieces of coated substrates. More recently, Lou and Huang[9] introduced a first-principle–based, integrated dynamic modeling approach that can be used to characterize coating dynamic behavior in industrial settings. The model predictions of coated panel temperature dynamics were very close to the real data. Their reactive drying model is ideal for further study of quality-constrained energy reduction.

The model-based dynamic optimization is very complex because the reactive drying of coating is a multistage, moving-boundary, distributed-parameter problem. Total energy minimization of the oven is not simply equal to the minimization of energy in individual zones. Likewise, the coating quality should be uniform for all individual vehicle panels but different panels usually experience different baking conditions (such as temperature dynamics, solvent removal dynamics, curing dynamics, etc.) in the same oven arising from their different locations and surrounding conditions. This can make many mathematical programming–based optimization techniques difficult to use. A number of rigorous dynamic optimization algorithms have been developed[10,11] for solving problems involving partial and ordinary differential equation (PDE and ODE) constraints. In this article, an enhanced *ant colony system* (ACS) optimization methodology will be introduced to tackle this type of optimization problems from a heuristic approach.

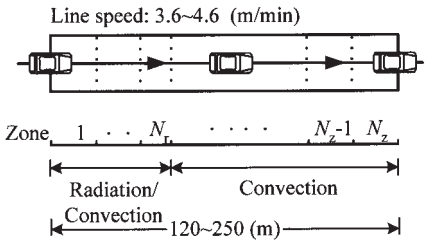

Figure 1. Sketch of a typical clearcoat oven-baking process.

The ant system optimization was first introduced by Dorigo et al.[12,13] for handling traveling salesman problems. It is a general-purpose heuristic algorithm that was inspired by the behavior of real ant colonies and, in particular, by their foraging behavior. It is a population-based algorithm that uses exploitation of positive feedback as well as greedy search. The effectiveness of its different versions as an optimization tool has been demonstrated in a number of applications,[14] which inspire us to attempt to solve dynamic optimization problems, such as this product-quality–constrained energy minimization problem.

The remainder of this article is organized in the following manner. First, a technique for integrating an integrated dynamic model into an optimization schema will be introduced. Then, ACS optimization basics and the extension of an existing ACS algorithm will be presented. A detailed case study will be followed to demonstrate the efficacy of the methodology. Finally, the applicability of the methodology in general dynamic optimization problems will be discussed and the advantages of the methodology will be summarized.

Dynamic-Model–Embedded Optimization

A typical clearcoat baking process is illustrated in Figure 1. Vehicle bodies covered by a thin layer of wet film move through the oven in sequence at a constant line speed that is determined by production rate. The oven is always divided into a number of zones so that different heating mechanisms can be applied with different settings.[15] In the oven, three types of interdependent phenomena occur simultaneously (Figure 2):

(1) Heat transfer on vehicle panels and within the thin film as a result of radiation, convection, and conduction

(2) Mass transfer of solvents through diffusion and evaporation that leads to the changes of film moisture content and film thickness

(3) Crosslinking reaction that causes the film-forming chemicals in paint to move and form a three-dimensional (3-D) molecular network

In this reactive drying, physical drying and chemical polymerization take place simultaneously. Chemical reactions occur with phase changes, such as gelation and vitrification. A detailed description of the clearcoat drying process can be found in Lou and Huang.[9]

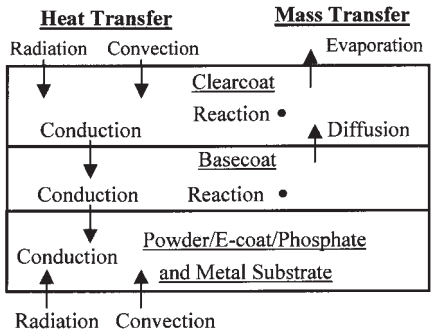

Figure 2. Heat- and mass-transfer and reaction mechanisms in different layers of coatings on vehicle panels.[9]

Product quality–constrained optimization problem

The reactive drying optimization targets the minimization of energy consumption in operation. This is subject to: (1) process constraints, such as those about the availability of materials, energy, air, and productivity; (2) integrated dynamic models that characterize the behavior of coatings on different panels under various operating conditions; (3) quality constraints, such as filmbuild and crosslinking reaction conversion; and (4) computational and mathematical constraints to ensure solution feasibility.

Energy minimization

As stated, the oven is divided into a number of zones with different lengths, and each zone may have different heating mechanisms (either radiation or convection, or both) and different parameter settings (such as oven wall or emitter temperatures, and air temperatures and velocities). The total oven energy is the sum of the energy consumed in the individual zones.

In an oven, the first few zones (usually two zones) have mainly radiation with high-energy flux; airflow in these zones is always very low to avoid dust in air landing on the wet film. The succeeding zones have convection only, including the last zone for cooling down (but with no energy needed). Thus, the optimization objective function can be defined as

$$\min Q = \sum_{i=1}^{N_r} Q_i^r + \sum_{i=1}^{N_z-1} Q_i^v \tag{1}$$

where N_r and N_z are the numbers of radiation zones and convection zones, respectively; Q_i^r and Q_i^v are, respectively, the radiation energy and the convection energy needed in the ith zone, and they can be evaluated by the following formulas:

$$Q_i^r = \sum_{j=1}^{N_p} \sum_{n_k=1}^{\mathrm{int}(t_i/\Delta t)} \frac{A_j \Im \sigma \varepsilon \Delta t e_r^{-1} [(T_i^w)^4 - T_{i,j}^4(n_k)]}{t_i}$$

$$i = 1, 2, \ldots, N_r \tag{2}$$

$$Q_i^v = \sum_{j=1}^{N_p} \sum_{n_k=1}^{\mathrm{int}(t_i/\Delta t)} \frac{h_{i,j} A_j e_v^{-1} \Delta t [T_i^a - T_{i,j}(n_k)]}{t_i}$$

$$i = 1, 2, \ldots, (N_z - 1) \tag{3}$$

where T_i^w and T_i^a are the wall and air temperature in the ith zone, respectively; e_r and e_v are the thermal efficiency of the radiation and the air convection, respectively; $T_{i,j}$ is the temperature of the jth panel in the ith zone; A_j is the surface area of the jth panel; $h_{i,j}$ is the heat transfer coefficient for the jth panel in the ith zone; t_i is the time required for a vehicle to pass through the ith zone. Discrete temperature $T_{i,j}(n_k)$ is used to calculate the energy consumed in each zone, and the temperature in each small time interval Δt is treated as a constant, which is the panel temperature at the beginning of the time interval.[16]

Constraints

The optimization is subject to three types of constraints: an integrated process dynamic model, coating quality, and solution feasibility.

Integrated Reactive Drying Model. The model by Lou and Huang,[9] directly adopted in this work, is listed in the Appendix; the detailed information about model development can be found in Lou and Huang.[9]

Coating Quality–Related Constraints. Various operation parameters are either directly or indirectly related to the eventual coating quality. These parameters are classified as follows.

- *Wall temperature*. In any zone, the wall temperature setting must be restricted to avoid the loss of control of panel heating. At the same time, this will prevent any unreasonable demand on the furnace that provides wall heating. Thus, the constraint is

$$T_i^w \le T_w^u \qquad i = 1, 2, \ldots, N_r \tag{4}$$

where T_w^u is the upper limit of the wall temperature and T_i^w is the wall temperature in the ith zone.

- *Convection air*. The convection air temperature and air velocity should be in specific ranges. For different zones, the air velocity limits may be different. In the radiation/convection zones, the maximum permissible air velocity is much lower than that in the succeeding convection-only zones. These suggest

$$T_{a_i}^l \le T_i^a \le T_{a_i}^u \tag{5}$$

$$V_{a_i}^l \le V_i^a \le V_{a_i}^u \tag{6}$$

where $T_{a_i}^l$ and $T_{a_i}^u$ are the lower and upper bounds of the air temperature in the ith zone, respectively; and $V_{a_i}^l$ and $V_{a_i}^u$ are the lower and upper limits of the air velocity in the ith zone, respectively.

- *Panel temperature*. In production, panel temperatures in different zones should be within specific ranges as well, that is,

$$T_i^l \le T_{i,j} \le T_i^u \tag{7}$$

where T_i^l and T_i^u are, respectively, the lower and upper bounds of the panel temperature in the ith zone.

• *Panel heating rate*. The temperature gradient of each panel at any time should not exceed the upper limit in each zone, that is,

$$\frac{dT_{i,j}}{dt} \leq \mu_{i,j}^T \tag{8}$$

where $\mu_{i,j}^T$ is the upper limit of temperature gradient of the jth panel in the ith zone.

Similarly, the temperature change when a vehicle moves from one zone to the next should also be restricted, that is,

$$\left| \frac{dT_{i,j}(t_i^e)}{dt} - \frac{dT_{i+1,j}(t_{i+1}^0)}{dt} \right| \leq \mu_{\Delta t} \tag{9}$$

where t_i^0 and t_i^e are, respectively, the starting and ending times of the ith zone; $\mu_{\Delta t}$ is the upper bound of temperature change rate between the two adjacent zones. When the vehicle moves into the last zone (that is, the cooling zone), this constraint does not apply.

• *Crosslinking conversion percentage and time window*. The final crosslinking conversion percentage should reach a desired value and last for a certain time period. This gives

$$r^l \leq c_{i,j}(t) \tag{10}$$

$$t^e - \Delta t_x \leq t \leq t^e \tag{11}$$

where r^l is the lower bound of the final conversion percentage, t^e is the time when the vehicle leaves the oven, and Δt_x is the minimum time required for holding the final crosslinking conversion percentage.

• *Drying rate*. The drying rate should be restricted to prevent the occurrence of certain types of defects. That is,

$$-\frac{d\bar{w}_{i,j}}{dt} \leq \mu_i^w \tag{12}$$

where $\bar{w}_{i,j}$ is the mean solvent content of the film on the jth panel in the ith zone (refer to the Appendix for further explanation in solvent removal model) and μ_i^w is the upper limit of drying rate in the ith zone.

Moreover, the solvent residue in the final dry film must be below a certain value and the thickness should be in a specific range. This means

$$\bar{w}_j^e \leq w^{e,u} \tag{13}$$

$$z^{e,l} \leq z_j^e \leq z^{e,u} \tag{14}$$

where $w^{e,u}$ is the maximum final mean solvent residue; and $z^{e,l}$ and $z^{e,u}$ are the lower and upper limits of the final film thickness, respectively.

Solution Feasibility Requirement. The following constraints are physically meaningful and mathematically necessary.

• *Nonnegative energy consumption*

$$Q_i \geq 0 \tag{15}$$

• *Nonnegative solvent residue, film thickness, and crosslinking conversion percentage*

$$\bar{w}_{i,j} \geq 0 \tag{16}$$

$$z_{i,j} \geq 0 \tag{17}$$

$$c_{i,j} \geq 0 \tag{18}$$

Optimization complexity

The product quality–constrained energy minimization problem defined above can be generalized as follows: given a set of initial conditions and necessary parameter values, find effectively and efficiently an optimal solution of a set of decision variables so that the specified objective function can be minimized while all constraints are satisfied. Although this optimization statement is as general as most optimization tasks, the problem complexity can be described below.

(1) It is a large-scale multistage dynamic optimization problem with a mixed set of sparse linear and nonlinear constraints. The objective function is time variant and is a sum of interdependent subobjective functions. Obviously, the sum of local optimization (stage based) does not guarantee global optimization for the overall system.

(2) The integrated product-process dynamic model consists of a set of submodels that are interacted between the process and the product, and among operational stages. Each submodel contains a set of more detailed models describing the dynamic performance of a number of parameters.

(3) The majority of the constraints is time dependent and expressed by either (ordinary or partial) nonlinear differential or integral equations.

It is conceivable that such a nonlinear problem may be difficult to solve using known nonlinear programming techniques and very likely there exist a variety of local optima in the solution space.[17] To identify an optimal solution effectively and efficiently, a modified *ant colony system* (ACS) optimization methodology is proposed in this work. Before describing the methodology, the basics of ACS are presented first.

Ant Colony System Basics

The natural metaphor on which an ACS algorithm is based is that of an ant colony.[12] It has been found that real ants are always capable of finding the shortest path from a food source to the nest without using visual cues. Ants can also adapt to environmental changes. For example, they can find the new shortest path once the original one is no longer the shortest because of the appearance of an obstacle.[18,19] It is known that ants can secrete a substance called "pheromone" and use its trial as a medium for communication among them. Each ant prefers probabilistically to follow the direction rich in pheromone. This explains why and how they can find the shortest path that reconnects a broken path after a sudden appearance of an unexpected obstacle has interrupted the initial path. As

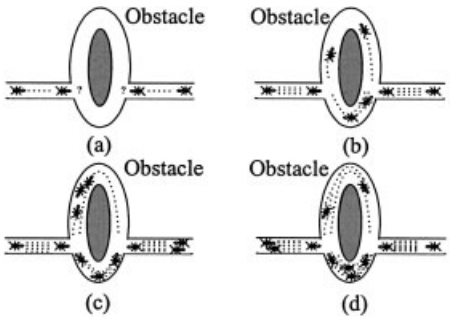

Figure 3. Path search by ants.[11]

shown in Figure 3a, where an obstacle has appeared, two ants are on the left and the right sides of the obstacle, respectively. Because they cannot continue to follow the pheromone trail, they have to choose to turn either right or left. In this situation, it is reasonable to expect half the ants, if they are there, to choose to turn right, whereas the other half choose to turn left. It is interesting to note that those ants that choose, by chance, the shorter path around the obstacle will reconstitute the interrupted pheromone trail more rapidly than those choosing the longer path. Thus, the shorter path will receive a greater amount of pheromone per unit time (see Figures 3b and 3c). The number of dashed lines is roughly proportional to the amount of pheromone that the ants have deposited on the ground. After a shorter transitory period, the difference in the amount of pheromone on the two paths is sufficiently large so as to influence the decision of new ants coming into the system (this is shown by Figure 3d).

The cooperative search behavior of ants has inspired the new computational paradigm for optimizing real-life system problems in basic and applied sciences. This is especially suitable for solving large-scale optimization problems that can be either hardly formulated rigorously or solved expensively. ACS is an attractive alternative for identifying superior solutions with reasonable computational effort. By mimicking the real ant's behavior, a group of artificial ants are introduced to search in parallel cooperatively for good solutions through pheromone-mediated communications.

The available ACS techniques are mainly for solving steady-state optimization problems, such as traveling salesman problems.[13] In the following section, a new ACS-based dynamic optimization methodology is detailed.

ACS-Based Optimization

The methodology will be presented in the following manner: a general optimization objective is introduced first, which is followed by detailed steps of solution search process. Then several rules adopted during the optimization are explained. Finally, an example will be given to facilitate the reader's understanding.

The goal of the optimization is to minimize the objective function, J, through optimizing the decision variable set, $\boldsymbol{X} \in R^N$, while all constraints should be satisfied. The optimal values of $\boldsymbol{X}$ form the vector $\tilde{\boldsymbol{X}}^{opt}$.

It is required that the initial values of $\boldsymbol{X}$ are given ($\tilde{\boldsymbol{X}}^0$), and for each variable, its permissible adjustment range is defined. Also assume that a group of M ants, denoted as set $\boldsymbol{A}$, participate in cooperative solution search, and the solution—either intermediate or final—identified by ant a_j is denoted by set $\tilde{\boldsymbol{X}}(a_j)$.

Solution search method

A solution identification process can be expressed by a set of search trees. Each tree corresponds with each variable and contains a number of nodes that are distributed in layers and a number of edges, each of which connects two nodes in two adjacent layers. All the ants will work on this set of search trees cooperatively. Each node represents a state (that is, a value) of a variable. The change of its state from one to the other is called state transition, or the transition between two nodes. In this text, a node is denoted as $n_{i,k,p}$, which is the kth node of the pth layer of the search tree for the ith variable, and the pheromone amount on an edge, which connects nodes $n_{i,j,p-1}$ and $n_{i,k,p}$ for the ith variable, is denoted as $\tau_{i,j,k,p}$. Note that a "node" represents each initial or candidate value for each decision variable, an "edge" refers to a transition from the initial value to a candidate value for one decision variable, and a "tour" is defined as a set of edges traversed by one ant for all variables from the initial points (not random, but a feasible solution) to the new settings (a new feasible solution).

In this method, each variable will be optimized jointly by M ants (a_j, $j = 1, 2, \ldots, M$). For simplicity, it is assumed that each layer of a search tree contains L nodes, representing L options for variable x_i. The search approach contains the following major steps.

Step 1. Initiate a new computation outer iteration, say the pth. Evaluate the sensitivity of each element x_i in $\boldsymbol{X}$ and develop vector $\boldsymbol{S} \in R^N$. The value of s_i (an integer between 1 and N) represents the prioritized sensitivity of decision variable x_i to the objective function. For instance, if s_5 equals 1, then x_5 is the most sensitive variable that is to be optimized first.

Step 2. Optimize variables in $\boldsymbol{X}$ in the sequence suggested by $\boldsymbol{S}$. An accomplishment of optimizing all variables in $\boldsymbol{X}$ once accounts for the completion of an inner iteration. Note that each outer iteration consists of two or more inner iterations. Each inner iteration will be accomplished by executing the following four substeps.

(1) *Step 2-1.* For the selected x_i, ant a_j starts at its current value $\tilde{x}_i^c(a_j)$ [that is, node $n_{i,j,p-1}$ that was derived from the $(p-1)$th layer] to search for an optimal value $\tilde{x}(a_j)$ (that is, node $n_{i,k,p}$ in the pth layer) using the state transition (ST) rule. Then, ant a_j updates the pheromone on edge $\tau_{i,j,k,p}$ using the local pheromone updating (LPU) rule.

(2) *Step 2-2.* Repeat Step $2-1$ M times so that each ant can identify its optimal value for x_i (a new node) and update the pheromone of the relevant edge.

(3) *Step 2-3.* For variable x_i, M ants generate M optimal values (they could be all same, or all different as two extremes), and they will remember their own choices for that variable.

(4) *Step 2-4.* After finishing all the variables, each ant finds an optimal solution $\tilde{\boldsymbol{X}}^{opt}$ for the problem. The solution by ant a_l giving the smallest value of J is the best and if this solution is better than existing solution, this newly identified set, $\tilde{\boldsymbol{X}}^{opt}$ is selected as the optimal. Moreover, in this layer, the pheromone of each edge of each tree will be reevaluated by the global

pheromone updating (GPU) rule. Then, begin another inner iteration from Step 2-1 in this pth outer iteration.

Step 3. Determine whether the identified $\tilde{\boldsymbol{X}}^{opt}$ is acceptable after finishing all inner iterations in one outer iteration. The acceptance criterion can be convergence based, the number of iterations based, and so on. If acceptable, $\tilde{\boldsymbol{X}}^{opt}$ is considered the final solution of $\boldsymbol{X}$, and the corresponding objective function value, $J(\tilde{\boldsymbol{X}}^{opt})$, is the minimum value. The optimization process can be terminated in this outer iteration. If the identified $\tilde{\boldsymbol{X}}^{opt}$ is not acceptable, then this $\tilde{\boldsymbol{X}}^{opt}$ will be the initial value for the next outer iteration starting from Step 1 again.

Solution identification rules

The search repeatedly uses a sensitivity sequence determination method and three rules: the state transition (ST) rule, the local pheromone updating (LPU) rule, and the global pheromone updating (GPU) rule. These are described below.

Assume that in each layer, $\tilde{\boldsymbol{X}}_i^c$ consists of those L discrete candidate values for variable x_i (notice that a different layer may have different values of $\tilde{\boldsymbol{X}}_i^c$). Thus it is clear that $\tilde{x}_i(a_j)$ is one value in set $\tilde{\boldsymbol{X}}_i^c$.

Sensitivity Sequence Determination. Given decision variable set $\boldsymbol{X} \in R^N$, introduce sensitivity sequence vector $\boldsymbol{S} \in R^N$. The sequence will be determined in two steps.

(1) *Step 1*. Evaluate the sensitivity of variable x_i using the following formula:

$$\phi_i = \left.\frac{\partial J}{\partial x_i}\right|_{\tilde{X}} \qquad i = 1, 2, \ldots, N \tag{19}$$

where J is the objective function and $\tilde{\boldsymbol{X}}$ contains the initial values of all variables except for x_i, which selects one of the candidate values for sensitivity evaluation. This will generate the sensitivity vector, $\boldsymbol{\Phi} \in R^N$.

(2) *Step 2*. Examine the magnitude of ϕ_i values. Assign "1" to s_i in $\boldsymbol{S}$ if ϕ_i is the largest in $\boldsymbol{\Phi}$; assign "2" to s_j if ϕ_j is the second largest, . . . , and finally, assign "N" to s_k if ϕ_k is the smallest. Vector $\boldsymbol{S}$ with all elements assigned gives the information about the sensitivity of each decision variable. Note that, if several decision variables have the same sensitivity, a search order for these variables can be random without reducing a chance of identifying a superior solution.

State Transition (ST) Rule. For selected x_i, ant a_j identifies its optimal value $\tilde{x}_i(a_j)$. This means that each ant should make a transition for x_i from the initial value $\tilde{x}_i^0$ to a candidate value in set $\tilde{\boldsymbol{X}}_i^c$. Assume $\tilde{x}_i^0$ is at node $n_{i,j,p-1}$; the nodes in the next layer are $n_{i,k,p}$, $k = 1, 2, \ldots, L$; and the pheromone of the edge between nodes $n_{i,j,p-1}$ and $n_{i,k,p}$ is denoted as $\tau_{i,j,k,p}$ assuming it is at the pth layer. Then, the state transition rule can be expressed by the following function:

$$d = \begin{cases} \arg\max\left\{\tau_{i,j,k,p}\left(\varphi_{n_{i,j,p-1},n_{i,k,p}}\right)^{\theta} \middle| k = 1, 2, \ldots, L\right\} \\ \qquad \text{if } q \le q_0 & \text{(20a)} \\ \mathrm{D} \qquad \text{otherwise} & \text{(20b)} \end{cases}$$

where d is the node chosen, D is an integer randomly chosen between 1 and L, and $\varphi_{n_{i,j,p-1},n_{i,k,p}}$ is a heuristic function defined as

$$\varphi_{n_{i,j,p-1},n_{i,k,p}} = \begin{cases} \tilde{J}^{-1}\big|_{n_{i,k,p}} & \text{if all constraints satisfied} \quad \text{(21a)} \\ f^{-1} & \text{otherwise} \quad \text{(21b)} \end{cases}$$

where $\tilde{J}\,|_{\,n_{i,k,p}}$ is the objective function value when the ant chooses node $n_{i,k,p}$ to move to; θ is a parameter that weighs a relative importance of the heuristic function to the pheromone; and f is a very large number acting as a penalty. Note that it is possible that a node, such as $n_{i,k,p}$, chosen by an ant violates one or more constraints of an optimization problem. This node will not be excluded in the candidate set. Instead, a penalty constant f is introduced, which means that some infeasible intermediate solutions may be tolerated during optimization because it may be possible that the infeasible solution will become feasible after succeeding transitions and eventually it may turn to be a better solution.

The final node d is chosen from L candidate nodes, $n_{i,k,p}$, $k = 1, 2, \ldots, L$, in the following way. First, generate randomly $q \in [0, 1]$ and then compare q with a preset parameter q_0 ($0 \le q_0 \le 1$). If, $q \le q_0$, then node d will be chosen based on Eq. 20a. Equation 20a is considered a greedy rule, which prefers the transition to the node giving a greater amount of pheromone and/or a smaller objective function value. However, if $q > q_0$, then a node will be randomly chosen based on the following probability evaluation with which an ant in node $n_{i,j,p-1}$ chooses node $n_{i,k,p}$ to move to

$$p_{n_{i,j,p-1},n_{i,k,p}} = \frac{\tau_{i,j,k,p}\left(\varphi_{n_{i,j,p-1},n_{i,k,p}}\right)^{\theta}}{\sum_{k=1}^{L} \tau_{i,j,k,p}\left(\varphi_{n_{i,j,p-1},n_{i,k,p}}\right)^{\theta}} \tag{22}$$

Note that in the pth layer, there exist L candidate nodes. Thus, L probabilities will be obtained using Eq. 22, and the sum of these values = 1. The selection of the final node, D, is based on the probability distribution.

Local Pheromone Updating (LPU) Rule. This rule is used repeatedly in Step 2-1, and it has the following iterative updating format:

$$\tau_{n_a,n_b} = \tau_{n_a,n_b} + \varpi(\tau_0 - \tau_{n_a,n_b}) \tag{23}$$

where $\varpi \in (0, 1)$ is the local pheromone decay parameter and τ_0 is an initial pheromone level. The above equation shows that if the current pheromone amount on one edge is $<\tau_0$, then the pheromone amount will be increased after applying this rule; otherwise, it will be decreased. Understandably, this rule gives ants more chance to explore new transitions to prevent premature convergence. In addition, if ϖ is very small, the pheromone does not change too much in each update. On the other hand, a large ϖ (that is, a severe decay) leads to a major change of the amount of pheromone. In a wide range, this rule can control the change of desired edges; the ants can make a better use of pheromone information. Without this local pheromone updating activity, ants would search only in a narrow neighborhood of the best available solution.

Global Pheromone Updating (GPU) Rule. Once all ants have finished transitions for all decision variables in $\boldsymbol{X}$, the

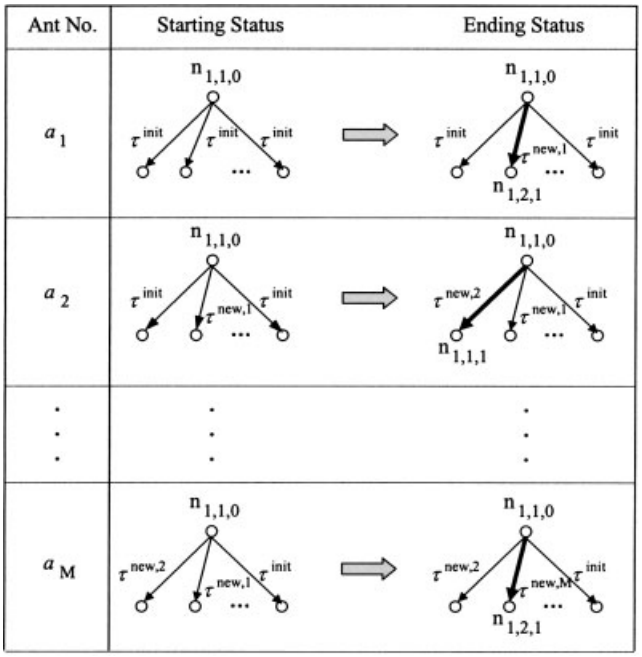

Figure 4. Identification of optimized values of variable x_1 by each ant using the state transition rule.

amounts of pheromone on the edges in the search trees in the current inner iteration should be updated using the following formula:

$$\tau_{n_a,n_b} = \begin{cases} \tau_{n_a,n_b} + \omega[(\tilde{J}^{opt})^{-1} - \tau_{n_a,n_b}] & \text{if } (n_a, n_b) \in \text{current best tour} \\ (1-\omega)\tau_{n_a,n_b} & \text{otherwise} \end{cases} \tag{24}$$

where $\omega \in (0, 1)$ is the global pheromone decay parameter and $\tilde{J}^{opt}$ is the minimum value of the objective function using $\tilde{X}^{opt}$. Note that only those edges giving the current best solution can increase their pheromone amounts, whereas all others need to have their pheromone amounts reduced. This rule helps identify a globally optimal solution more quickly. Note that, in search, the algorithm always needs to pick the "current best one," but the system would not tend to preserve any local optima. Instead, the solution diversity in the ACS algorithm is accomplished by (1) distributed computation, (2) pseudo-random-proportional rule, (3) infeasible solution tolerance, (4) local pheromone updating rule, and (5) searching space updating. These measures will allow the optimization process to move out from the current best solution.

Solution search example

The search method can be understood by the example shown in Figures 4 through 6. In Figure 4, a process of identifying optimal values for variable x_1 by M ants in the first inner iteration of search is illustrated. In this example, a_1 starts the search first at node $n_{1,1,0}$, and the initial pheromone on all edges are set to the same (τ^{init}). The search results in the identification of the optimal value $\tilde{x}_1(a_1)$ (that is, node $n_{1,2,1}$). The pheromone of edge $\tau_{1,1,2,1}$ is changed from τ^{init} to $\tau^{new,1}$ by the LPU rule, whereas all other edges have no pheromone change. In the resulting tree, ant a_2 starts the search at node $n_{1,1,0}$ and it ends in node $n_{1,1,1}$. Correspondingly, only $\tau_{1,1,1,1}$ is changed to $\tau^{new,2}$. The search will be ended by the effort of a_M. The best node identified by a_M is $n_{1,2,1}$. The pheromone of edge $\tau_{1,1,2,1}$ only is changed to $\tau^{new,M}$.

The search generates M optimal values, $\tilde{x}_1(a_j)$ ($j = 1, 2, \ldots, M$), which can be all the same or all different as the two extreme cases. Each $\tilde{x}_1(a_j)$ will be remembered by each ant a_j and will be used by that ant in the process of making transitions for the next variables. Note that the pheromone amounts on those edges, which connect $n_{1,1,0}$ and optimal nodes, have been updated.

Figure 5 depicts the first two outer iterations (suppose only one inner iteration in each outer iteration) of the solution search for all N variables. In each iteration, all ants optimize all the variables according to a certain sequence. As shown in the resultant trees after Iteration 1, node $n_{1,1,1}$ for variable x_1, node $n_{2,L,1}$ for variable x_2, . . . , and node $n_{N,2,1}$ for variable x_N are the best. This means that variables $x_1, x_2, \ldots, x_N$ have their values changed from $\tilde{x}_1^0, \tilde{x}_2^0, \ldots, \tilde{x}_N^0$ to $\tilde{x}_1^1, \tilde{x}_2^1, \ldots, \tilde{x}_N^1$, respectively. Nodes $n_{1,1,1}, n_{2,L,1}, \ldots, n_{N,2,1}$ become the initial nodes for the search in Iteration 2. As shown, this new iteration leads to the identification of new optimal values of $x_1, x_2, \ldots, x_N$ at nodes $n_{1,2,2}, n_{2,1,2}, \ldots, n_{N,L,2}$, respectively. These optimal values and the evaluated objective function value will be considered the optimal solution for Iteration 2. $\tilde{X}^{opt}$ will be updated once an ant finds a better solution.

Based on the solution from Iteration 2, the need for a new iteration search will be determined. Figure 6 illustrates a complete solution search involving p outer iterations (shown results are for last inner iteration in each outer iteration). Finally, the solution for variables $x_1, x_2, \ldots, x_N$ are located at nodes $n_{1,2,p}, n_{2,L,p}, \ldots, n_{N,1,p}$.

Case Study: Quality Constrained Energy Optimization

The reactive drying process studied in this section has already been depicted in Figure 1. The oven is 125 m long and consists of seven zones: two radiation/convection zones, four convection-only zones, and one cooling zone. The zone length specification is listed in the first two columns of Table 1. Vehicle bodies move through the oven one by one at a constant speed. Each vehicle body has seven coated panels: hood, deck, roof, left and right sides, and left and right sills. The optimization model developed in this work is used to optimize this specific oven for quality-constrained energy minimization.

As discussed previously, the problem in this work is sufficiently constrained and the objective in the case study is improvement of current system performance. The proposed ACS methodology will not generally cause the loss of solution feasibility because it starts from an industrial setting (already located in the feasible solution space), and once a set of new solutions is constructed, the feasibility will be assessed immediately and infeasible solutions will be rejected.

Process specification

Three types of parameters should be specified before optimization.

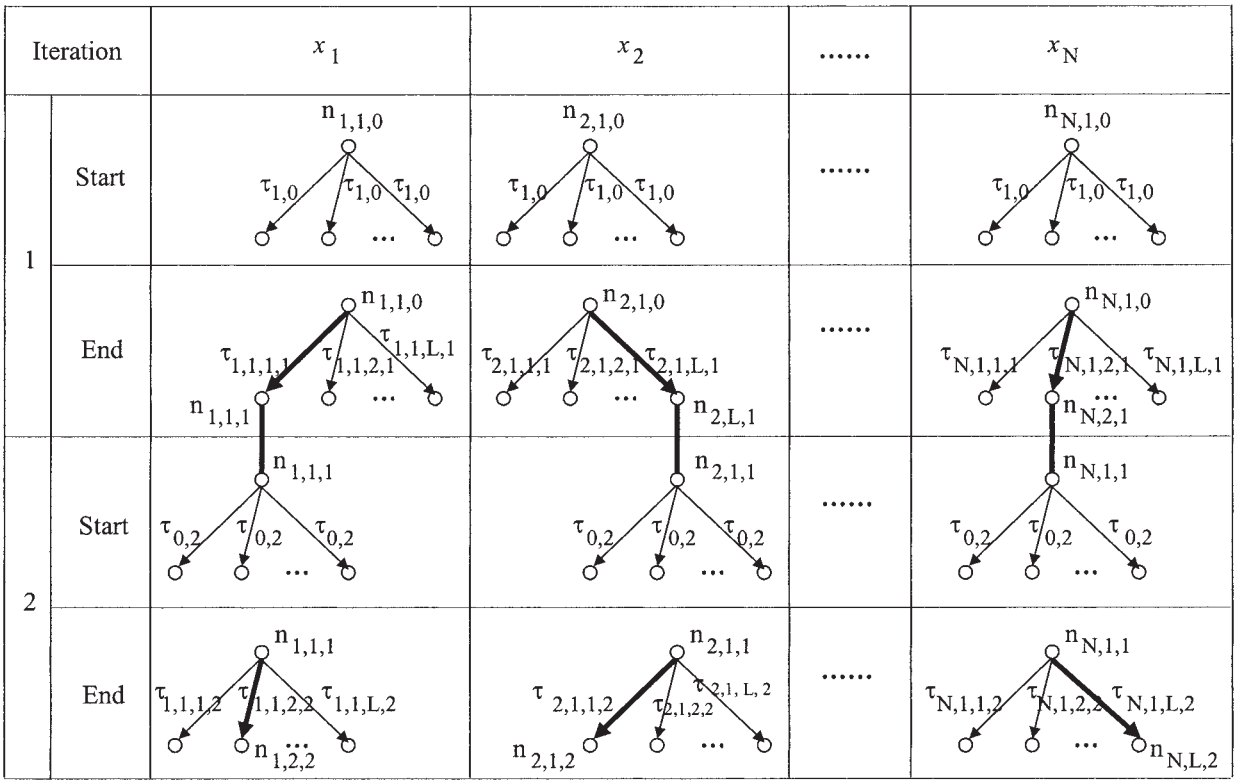

Figure 5. First two iterations of multivariable solution search using the ACS algorithm.

(1) *Parameters of the integrated dynamic model*. The original operation settings of the wall temperature, convection air temperature, and velocity of each zone (except for the last cooling zone) are listed in columns 3 and 4 of Table 1. These settings are industrial data that were used in a real process. Each vehicle body, initially at 300 K for each panel, moves through the oven at the line speed of 0.069 m/s. It is assumed that the wet clearcoat on the vehicle surface has a solvent content of 0.18 and initial thickness of 70 μm. In calculation, the film is divided horizontally into 14 slices. The panel thick-

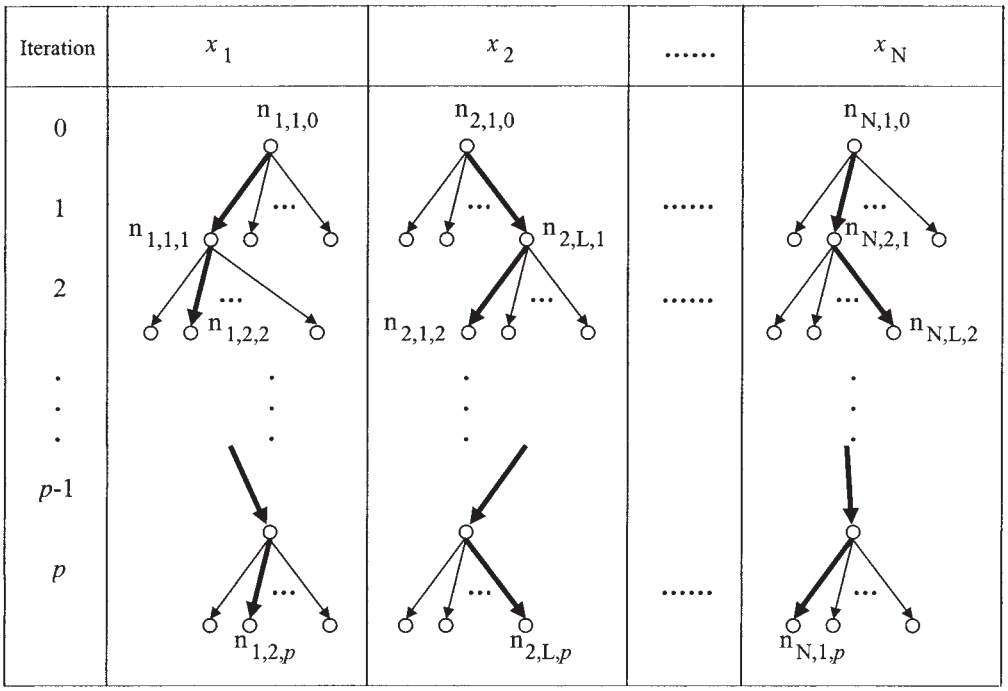

Figure 6. Iterative search for optimal values of all decision variables.

Table 1. Comparison of Process Settings before and after Optimization

Zone No.	Zone Length (m)	Original V^a (m/s)	Original T^w, T^a (K)	Optimal (ACS) V^a (m/s)	Optimal (ACS) T^w, T^a (K)	Optimal (GA) V^a (m/s)	Optimal (GA) T^w, T^a (K)
1	20.73	0.18	473, 403	0.29	500, 397	0.18	500, 404
2	13.41	0.18	478, 478	0.16	500, 435	0.16	500, 462
3	23.67	1.8	—, 428	1.53	—, 430	1.80	—, 427
4	23.67	1.8	—, 423	1.47	—, 426	1.79	—, 423
5	23.67	1.8	—, 418	2.27	—, 415	2.13	—, 415
6	10.54	1.8	—, 418	2.25	—, 414	1.13	—, 396
7	9.14	3.5	—, 300	3.5	—, 300	3.40	—, 292
Energy (kWh)		289.92		258.87		261.32	

ness is 3 mm. The heat-transfer coefficient is set to 5–50 W m^{-2} K^{-1}. The time interval is 20 s. The densities of the solid and solvent of the paint are 1.2×10^3 and 1.0×10^3 kg/m^3, respectively. To simulate the process, the constants γ, η, and ζ in the model are set to 0.332, 9.38×10^{-6} m^2/s, and 5×10^{14} s^{-1}, respectively, and the activation energies for diffusion and reaction, E_d and E_r, are 2.27×10^4 and 1.1356×10^5 J/mol, respectively. Emissivity ε is set to 0.4. The surface areas and viewing factors for radiation are different for different panels.

(2) *Constraints*. In operation, it is required that the temperature of any panel should not exceed 470 K, and the wall temperature and air temperature should not exceed 500 K. The air velocities in zones 1 and 2 should be <0.3 m/s and those in zones 3–6 <2.3 m/s. To have a desirable crosslinking structure of the dried film, the polymerization conversion percentage should eventually be >90% and last at least 5 min for each panel. To prevent defects caused by improper heating, the temperature increment of the panels cannot exceed 16 K/min, the film drying rate must be <0.0035 s^{-1}, and the temperature transition between two consecutive zones should be <7.8 K/min. For the dry film, the solvent content should be <0.03, and the film thickness must be in the range of 53.3 ± 5.1 μm.

(3) *Parameters for the ACS algorithm*. In solution search, a total of 10 ants are developed. In each search layer, the number of candidate values of each variable is 26. This defines the search region in each transition. For the temperatures, 10 K above and 15 K below the initial values are used as the upper and lower limits, respectively. For the velocities, 0.1 m/s above and 0.15 m/s below the initial velocity are used for the upper and lower limits, respectively. The number of search iterations and the number of inner iterations are set to 60 and 2, respectively. In addition, the constants θ, ϖ, ω, and q_0 are set to 3, 0.1, 0.1, and 0.5, respectively.

Based on the initial setting, the base energy consumption is 289.92 kWh (see Table 1). In the ACS algorithm, the initial pheromone amount for each edge is $\tau_0 = (N \times \tilde{J})^{-1}$, where N is the number of decision variables, which is 14 in this case and $\tilde{J}$ is the initial objective function value in each outer iteration.

Note that the 14 decision variables, that is, the wall temperature and air temperature in each zone, and the air velocity in each zone, are continuous variables in the original formulation. It needs to be pointed out that tree-based search algorithms, including ACS, appears only to be applicable to discrete decision variables. To solve this case study problem using ACS, the continuous differential-algebraic equation (DAE) and PDE constraints were discretized. The temperature and the air velocity variables were discretized as well. Specifically, 1 K and 0.01 m/s were used as the intervals for the discretization of the temperature and the air velocity, respectively. This "coarse" scheme is sufficient for the optimization and control of automotive clearcoat drying process according to industrial practice. Through the discretization, each decision variable has about 50 candidate discrete values in total.

Optimization procedure of applying ACS algorithm

The three-step optimization procedure is used to identify an optimal settings of the oven. Figure 7 together with Table 2 give a clear illustration of the optimization process.

Figure 7 shows the initial operation parameter settings for this process. The wall temperature, air temperature, and velocity in each zone are decision variables, giving a total of 14 variables x_i, $i = 1, 2, \ldots, 14$. T^p and T^d are defined as the search region of the temperatures and V^p and V^d are for each velocity variable in one iteration.

Table 2 lists the detailed results by ant a_1 in finding a complete solution during the first inner iteration of the optimization. Using industrial settings in row 3 of the table, the sensitivity sequence vector $\boldsymbol{S}$ for this iteration is shown in row 2 of Table 2. As shown, the air temperature in the sixth zone (T_6^a, that is, x_{13}) is the most sensitive variable. Thus, all the ants make transitions first for this variable by applying the ST rule. Note that when the objective function value is evaluated, the value for T_6^a is chosen from its candidate values, but values for the other variables just keep the original settings. In this table, a_1 chooses 416 K for T_6^a at last. Then the pheromone amount on the edge connecting nodes 418 K with 416 K for variable T_6^a will be updated by the LPU rule (see row 4 of the table). The

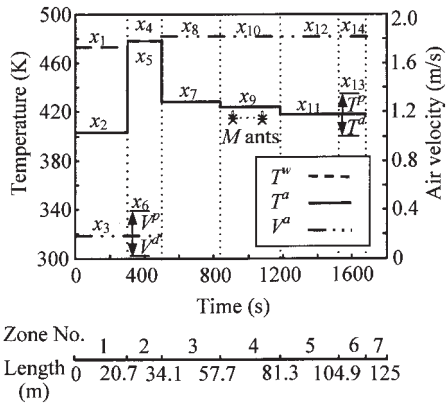

Figure 7. Initial operation parameter settings of the oven.

Table 2. An Example of Solution-Construction Process by One Ant

Zone-Based Optimization Parameters ($\boldsymbol{X}$)	Zone 1			Zone 2			Zone 3		Zone 4		Zone 5		Zone 6	
	x_1 T_1^w	x_2 T_1^a	x_3 V_1^a	x_4 T_2^w	x_5 T_2^a	x_6 V_2^a	x_7 T_3^a	x_8 V_3^a	x_9 T_4^a	x_{10} V_4^a	x_{11} T_5^a	x_{12} V_5^a	x_{13} T_6^a	x_{14} V_6^a
Sequence ($\boldsymbol{S}$)	4	10	8	5	6	2	9	11	7	12	3	14	1	13
Initial value ($\tilde{\boldsymbol{X}}^0$)	473	403	0.18	478	478	0.18	428	1.8	423	1.8	418	1.8	418	1.8
1st transition	SV*	SV	SV	SV	SV	SV	SV	SV	SV	SV	SV	SV	416	SV
2nd transition	SV	SV	SV	SV	SV	0.26	SV	SV	SV	SV	SV	SV	CV**	SV
3rd transition	SV	SV	SV	SV	SV	CV	SV	SV	SV	SV	416	SV	CV	SV
⋮	⋮	⋮	⋮	⋮	⋮	⋮	⋮	⋮	⋮	⋮	⋮	⋮	⋮	⋮
Last transition	CV	CV	CV	CV	CV	CV	CV	CV	CV	CV	CV	1.81	CV	CV
Complete solution	473	402	0.06	488	480	0.26	430	1.65	428	1.65	416	1.81	416	1.90

*SV: the same value kept.
**CV: the changed value kept.

other ants will also get their own optimal values for T_6^a in the same way. Then, all ants will optimize the second most sensitive variable V_2^a (that is, x_6). The only difference with the first transition is that, instead of using the initial value for the variable that has been optimized, the optimal values for T_6^a obtained by each ant will be adopted to evaluate the objective function value. In this table, 0.26 is chosen by a_1 for V_2^a (see row 5 of the table). After 14 transitions, a_1 obtains a complete solution, which is the result obtained by optimizing all the variables (see the last row of the table). In the same way, 10 ants will give 10 complete solutions. These solutions are then compared to find the optimal one in this iteration. Then the GPU rule will be applied. As mentioned before, the optimization process will continue until a final solution is achieved.

Solution analysis

To measure the performance of the proposed ACS method, another approach based on Genetic Algorithm (GA)[20] is implemented for comparison. Table 1 lists the original vs. optimal temperature and air velocity settings for each zone derived from both the ACS and the GA algorithms. It is observed from Table 1 that ACS outperformed GA in terms of solution quality. By comparing to the base case, new settings obtained from ACS and GA reduce the overall energy consumption in the oven to 258.87 kWh (10.74% reduction) and 261.32 kWh (9.8% reduction), respectively. Note that the results were calculated under the assumption of ideal condition and the variations of process parameters were not considered. The main purpose of this work is to propose and demonstrate an alternative dynamic optimization method to solve complex system problems. Thus, these variations were not considered at this stage.

Figure 8 shows the temperature and conversion percentage profiles for all seven panels before the optimization. Because of symmetry, the profiles of the right side are not differentiable from those of the left side, so as to hood and deck or right side sill and left side sill. To show the validity of the integrated reactive drying model, Figure 9 compares the filtered temperature profile from the industrial data for different panels with the profiles obtained from model prediction. Apparently, the model predictions are very acceptable.

Detailed system simulations were conducted using settings suggested by ACS. Figure 10 gives the comparison of dynamic profiles of all these panels before and after optimization. For example, Figure 10a shows both the temperature and the conversion percentage profiles before and after optimization for the left and the right sills. There are no noticeable changes for the solvent removal and film thickness after optimization. As shown in these figures, all the constraints are satisfied after the optimization. Thus with this optimal setting, the energy will be saved and at the same time, the quality of coating can be ensured.

Computational efficiency

Computational efficiency is always a concern when solving a complex system optimization problem. In this study, compu-

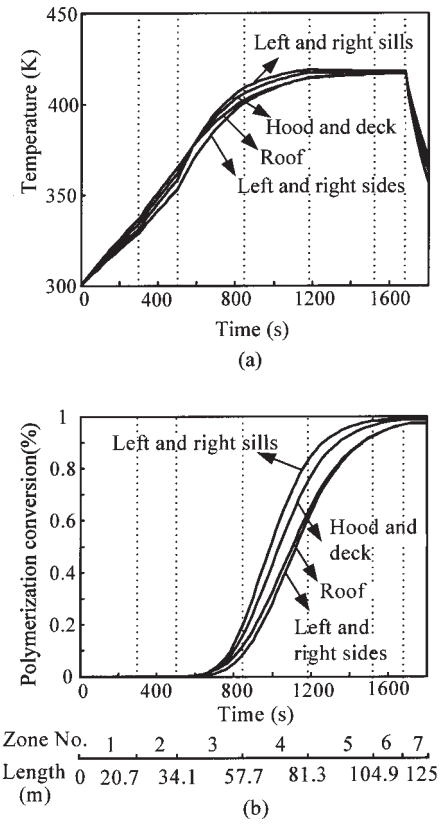

Figure 8. Panel temperature and crosslinking conversion profiles before the optimization.

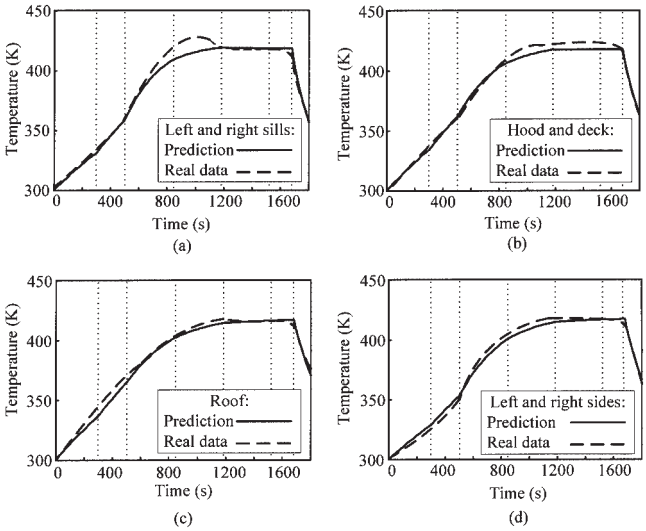

Figure 9. Temperature profiles of the panels.

tational time is monitored automatically. The ACS optimal results were obtained in outer iteration 12, and the total computational time is 1.04 h on a single CPU desktop (2.39 GHz). Figure 11 demonstrates a solution convergence comparison for the ACS and GA cases. It is shown that to have an equivalent solution as GA derived, ACS needs to spend about 15 min, which is about 3 min longer than that GA used. This type of solution revolution plot can help users to determine effectively when the optimization process should be terminated.

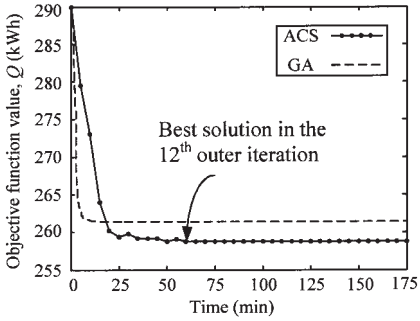

Figure 11. Solution revolution comparison.

Concluding Remarks

Clearcoat drying and curing in an oven is a complicated reactive drying process. In plants, the oven operational settings are basically experience based, which has caused various coating quality problems and higher energy consumption. By facing the difficulties in using conventional mathematical programming–based dynamic optimization methods, this article has introduced a nonconventional ant colony system (ACS)–based dynamic optimization methodology. The methodology significantly extends the original version of ACS from solving steady-state optimization problems to handling dynamic optimization problems. As demonstrated in the case study, this methodology is applicable to multistage, moving-boundary, multivariable optimization problems constrained by various linear and nonlinear differential and integral equations. ACS can derive a better solution than that obtained by conventional

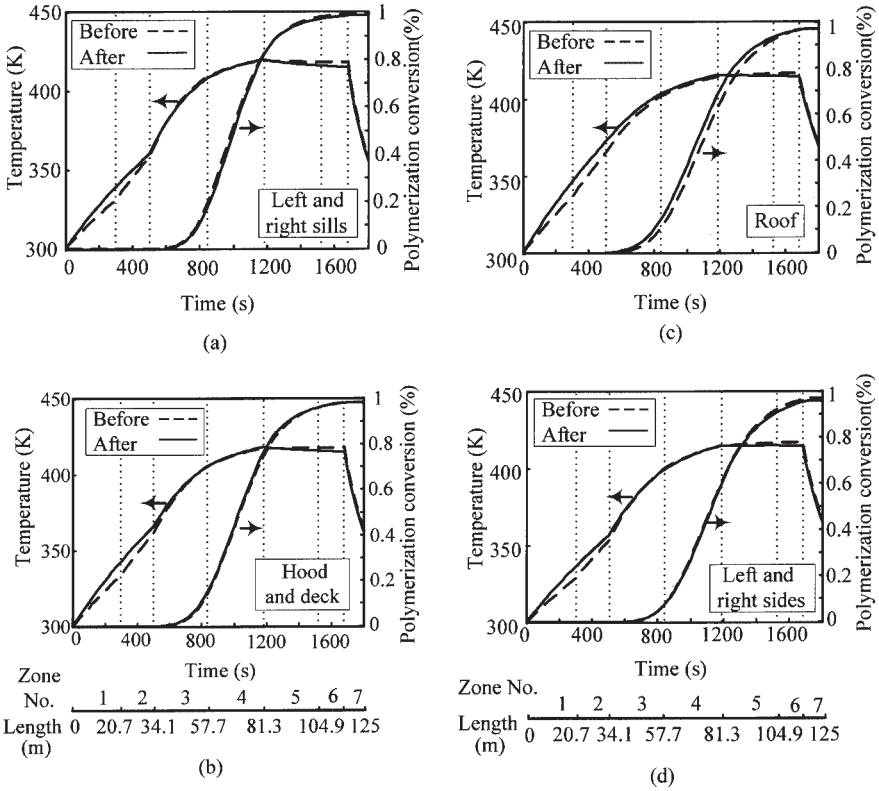

Figure 10. Temperature and crosslinking conversion profiles before and after optimization.

GA, although the computational efficiency needs further improvement.

With respect to the application, this methodology can give very attractive energy reduction benefits without any capital investment. A more attractive feature is that this methodology allows a close watch of product quality for any energy reduction attempt. This suggests that the complex coating quality control can no longer be based on postprocess inspection; it may become a reality that the coating quality assurance is integrated in every step of the curing operation. Thus, the energy needed for reworking unqualified coating in ovens can be significantly reduced or even eliminated.

Acknowledgments

This work was supported in part by the National Science Foundation (Grant CTS 0091398) and the Institute of Manufacturing Research of Wayne State University. Technical assistance from Ford Advanced Manufacturing Technology Development Center is also gratefully acknowledged.

Notation

A = surface area, m^2
c = monomer fractional conversion degree
C_p^m = heat capacity of panel metal, J kg^{-1} K^{-1}
D_f = diffusivity, m^2/s
e_r = energy efficiency for radiation
e_v = energy efficiency for convection
E_d = activation energy for diffusion, J/mol
E_r = activation energy for reaction, J/mol
h = heat transfer coefficient, W m^{-2} K^{-1}
K = mass-transfer coefficient, kg m^{-2} s^{-1}
N_p = number of panels of a vehicle
N_r = number of zones with radiation in an oven
N^s = number of film slices
N_z = number of total zones of an oven
P_a = pressure of convection air, Pa
P_s = saturation vapor pressure of solvent, Pa
Q = total energy consumption, kW
Q^r = radiation energy, kW
Q^v = convection energy, kW
R = gas constant, 8.314 Pa m^3 mol^{-1} K^{-1}
t = time, s
Δt = time interval, s
T = panel and film temperature, K
T^a = convection air temperature, K
T^w = oven wall temperature, K
V^a = convection air velocity, m/s
w = solvent content in film, kg solvent/kg solids in paint
$\bar{w}$ = mean solvent content in film, kg solvent/kg solids in paint
z = thickness of the film, m
z^m = thickness of panel metal, m
z^s = thickness of solids in paint, m
Δz = film thickness of each slice, m

Greek letters

α = activity constant of solvent
β = constant
γ = constant
ε = emissivity
ζ = polymerization reaction frequency factor, s^{-1}
η = preexponential constant for diffusion, m^2/s
θ = parameter of relative importance of pheromone vs. heuristic weight
ρ^l = density of solvent in paint, kg/m^3
ρ^m = density of panel metal, kg/m^3
ρ^s = density of solids in paint, kg/m^3
σ = Stefan–Boltzmann constant, 5.67×10^{-8} W m^{-2} K^{-4}
τ = pheromone amount
φ = heuristic weight for choices
ω = pheromone decay parameter for global updating
ϖ = pheromone decay parameter for local updating
$\Im$ = viewing factor for radiation

Literature Cited

1. Cohen ED, Gutoff EB. *Modern Coating and Drying Technology.* New York, NY: VCH Publishers; 1992.
2. Gutoff EB, Cohen ED. *Coating and Drying Defects.* New York, NY: Wiley; 1995.
3. Lou HH, Huang YL. Hierarchical decision support for defect reduction in automotive paint applications. *Eng Appl Artif Intel.* 2003;16:237-250.
4. Navarri P, Andrieu J. High-intensity infrared drying study. Part II. Case of thin coated films. *Chem Eng Process.* 1993;32:319-325.
5. Blanc D, Vessort S, Laurfnt P, Gerard JF, Andrieu J. Study and modeling of coated car painting film by infrared or convective drying. *Drying Technol.* 1997;15:2303.
6. Dickie RA, Bauer DR, Ward SM, Wagner DA. Modeling paint and adhesive cure in automotive applications. *Prog Org Coat.* 1997;31:209-216.
7. Howison SD, Moriarty JA, Ockendon JR, Terrill EL, Wilson SK. A mathematical model for drying paint layers. *J Eng Math.* 1997;32:377-394.
8. Hugget A, Sebastian P, Nadeau JP. Global optimization of a dryer by using neural networks and genetic algorithms. *AIChE J.* 1999;45:1227-1238.
9. Lou HH, Huang YL. Integrated modeling and simulation for improved reactive drying of clearcoat. *Ind Eng Chem Res.* 2000;39:500-507.
10. Biegler LT, Grossmann IE. Retrospective on optimization. *Comput Chem Eng.* 2004;28:1169-1192.
11. Kameswaran S, Biegler LT, Staus GH. Dynamic optimization for the core-flooding problem in reservoir engineering. *Comput Chem Eng.* 2005;29:1787-1800.
12. Dorigo M, Maniezzo V, Colorni A. Ant system: Optimization by a colony of cooperating agents. *IEEE Trans Syst Man Cybern B: Cybern.* 1996;26:29-41.
13. Dorigo M, Gambardella LM. Ant colony system: A cooperative learning approach to the traveling salesman problem. *IEEE Trans Evol Comput.* 1997;1:53-66.
14. Dorigo M, Gambardella LM. Guest editorial special section on ant colony optimization. *IEEE Trans Evol Comput.* 2002;6:317-319.
15. Koleske JV. *Paint and Coating Testing Manual.* West Conshohocken, PA: ASTM Publishing Services; 1995.
16. Seborg DE, Edgar TF, Mellichamp DA. *Process Dynamics and Control.* New York, NY: Wiley; 1989.
17. Edgar TF, Himmelblau DM, Lasdon LS. *Optimization of Chemical Processes.* New York, NY: McGraw-Hill; 2001.
18. Goss S, Aron S, Deneubourg JL, Pasteels JM. Self-organized shortcuts in the Argentine ant. *Naturwissenschaften.* 1989;76:579-581.
19. Beckers R, Deneubourg JL, Goss S. Trails and U-turns in the selection of the shortest path by the ant lasius niger. *J Theor Biol.* 1992;159:397-415.
20. Chipperfield AJ, Fleming PJ, Fonseca CM. Genetic algorithm tools for control systems engineering; 1994. http://www.shef.ac.uk/content/1/c6/03/35/06/intro_paper_2.pdf

Appendix: Integrated Reactive Drying Model

The integrated reactive drying model by Lou and Huang[9] adopted in this work is briefly presented below. More detailed information about model can be found in Lou and Huang.[9]

Panel heating model

The panel temperature dynamics can be described as follows. For the radiation/convection zone, the model is

$$\rho_j^m C_{p_j}^m Z_j^m \frac{dT_{i,j}}{dt} = \Im\sigma\varepsilon[(T_i^w)^4 - T_{i,j}^4] + h_{i,j}(T_i^a - T_{i,j}) \qquad i = 1, 2, \ldots, N_r \quad \text{(A1)}$$

where

$$h_{i,j} = \beta_{i,j}(V^a_{i,j})^{0.7} \tag{A2}$$

For the convection-only zone, the above model can be simplified as

$$\rho^m_j C^m_{p_j} Z^m_j \frac{dT_{i,j}}{dt} = h_{i,j}(T^a_i - T_{i,j}) \qquad i = (N_r + 1), 2, \ldots, N_z \tag{A3}$$

where ρ^m, C^m_p, and Z^m are density, heat capacity, and the thickness of the metal substrate, respectively (it is assumed that the paint has the same temperature as that of the related vehicle panel, and the mass of paint is negligible compared with that of the metal panel); $\Im$ is the viewing factor for radiation; σ is the Stefan–Boltzmann constant; ε is the emissivity; h is the heat transfer coefficient, which is a function of convection air velocity (V^a), the distance between the panel and the convection air nozzles; and other factors (expressed by β).

Solvent removal model

The following model can reveal that the solvent (or water) removal process occurred on the surface and within the clearcoat. To facilitate the modeling, we can divide the clearcoat film into a number of very thin slices, each of which has a fixed thickness (Δz). The total number of slices will be

$$N^s_j = \text{int}\left(\frac{z_j}{\Delta z}\right) \tag{A4}$$

The slices are numbered starting from the one just above the basecoat surface. There is no mass transfer from the basecoat beneath the clearcoat to the first slice of clearcoat because that basecoat is already dried when entering the oven. The mass change in the slice equals the solvent diffusion from the first slice to the second, that is,

$$\Delta z \frac{\partial w_{i,j,k}}{\partial t} = D_{f_{i,j,k}} \frac{\partial w_{i,j,k}}{\partial z} \qquad k = 1 \tag{A5}$$

where $w_{i,j,k}$ is the solvent content in the kth slice of the film on the jth panel in the ith zone. Note that the diffusivity D_f, which is dependent on the film temperature and solvent content, can be expressed as

$$D_{f_{i,j,k}} = \eta e^{-[(\gamma/w_{i,j,k}) + (E_d/RT_{i,j})]} \qquad k = 1, 2, \ldots, N^s_j \tag{A6}$$

where η is a preexponential constant for diffusion, γ is a constant, and E_d is the activation energy for diffusion.

For any slice from the second to the $(N^s_j - 1)$th, the change of solvent content is caused by the diffusion from the slice below to it and that from it to the slice above. This relationship can be expressed as

$$\frac{\partial w_{i,j,k}}{\partial t} = \frac{\partial}{\partial z}\left(D_{f_{i,j,k}} \frac{\partial w_{i,j,k}}{\partial z}\right) \qquad k = 2, 3, \ldots, (N^s_j - 1) \tag{A7}$$

For the top slice, the drying rate is defined as the change of mean solvent loss over time; it is controlled by solvent evaporation to the surroundings. The evaporation is largely determined by the solvent partial pressure as well as the mass-transfer coefficient (K). This relationship can be described as

$$\rho^s_j z^s_j \frac{\partial w_{i,j,k}}{\partial t} = K \frac{(P_a - \alpha P_s)}{P} + \rho^s_j D_{f_{i,j,k}} \frac{\partial w_{i,j,k}}{\partial z} \qquad k = N^s_j \tag{A8}$$

where ρ^s_j and z^s_j are, respectively, the density and thickness of unreducible components in the film of the jth panel.

Film thickness model

The film thickness decreases as the solvent is being removed. Different from the solvent removal model, this model contains the following integral equations for each panel:

$$\rho^l_j[z_j(t) - z_j(t + \Delta t)] = \rho^s_j\left[\int_0^{z_j(t)} w_j(t)dz - \int_0^{z_j(t+\Delta t)} w_j(t + \Delta t)dz\right] \tag{A9}$$

where ρ^l_j and ρ^s_j are densities, respectively, of solvent and unreducible components in the film of the jth panel. In this equation, the first and the second terms on the right-hand side represent the total moisture contents in the film of the jth panel at time t and $t + \Delta t$, respectively, if each term is multiplied by the surface area of that panel.

Polymerization model

The crosslinking reactions occurring in the film are rather complex. According to Dickie et al.,[6] the following first-order kinetic model can capture the major phenomena of the coating of each panel when it is baked:

$$\frac{dc_{i,j}}{dt} = \zeta e^{-E_r/RT_{i,j}}(1 - c_{i,j}) \tag{A10}$$

where $c_{i,j}$ is the polymerization conversion of the film on the jth panel in the ith zone, E_r is the reaction activation energy, and ζ is the reaction frequency factor.

Manuscript received Oct. 19, 2004, revision received Sep. 10, 2005, and final revision received Nov. 14, 2005.